Articles

A Large Deletion in the Connection Subdomain of Murine Leukemia Virus Reverse Transcriptase or Replacement of the RNase H Domain with *Escherichia coli* RNase H Results in Altered Polymerase and RNase H Activities†

Klara Post,‡ Jianhui Guo,‡,§ Eva Kalman,‡ Tsuneko Uchida,‖ Robert J. Crouch,‡ and Judith G. Levin*,‡

Laboratory of Molecular Genetics, National Institute of Child Health and Human Development, National Institutes of Health, Bethesda, Maryland 20892, and Mitsubishi Kasei Institute of Life Sciences, Tokyo 194, Japan

Received January 20, 1993; Revised Manuscript Received March 15, 1993

ABSTRACT: The functional relationship between the polymerase and RNase H domains of reverse transcriptase (RT) was investigated by studying the activities of AKR murine leukemia virus (MuLV) enzymes. In addition to the wild type, an RNase H-minus RT missing the entire RNase H domain and two other mutants having abnormal polymerase:RNase H ratios were expressed. These mutants include (i) a chimeric protein in which the MuLV RNase H domain was replaced by the entire *Escherichia coli* RNase H sequence and (ii) an RT with a 126 amino acid deletion in a region analogous to the "connection" subdomain in the p66 subunit of human immunodeficiency virus type 1 RT (Kohlstaedt, L. A., Wang, J., Friedman, J. M., Rice, P. A., & Steitz, T. A. (1992) *Science 256*, 1783–1790). With the wild-type RT, the major RNase H cleavage reaction was coordinated with DNA synthesis and occurred at a position corresponding to 15 nucleotides from the 3′-terminus of the DNA primer. Additional cleavages closer to the 5′-end of the RNA were explained in terms of a model relating binding of the RNA·DNA hybrid substrate and enzyme structure. The chimeric RT behaved like *E. coli* RNase H, exhibited 300-fold higher RNase H activity than wild-type RT, and was limited in its ability to synthesize DNA. Qualitative and quantitative changes in the polymerase and RNase H activities of the deletion mutant were also observed. The RNase H domain appeared to function independently of the polymerase domain, supporting the idea that the proper spatial relationship between the two active centers was disrupted by the mutation. Taken together, our results indicate that alteration of the normal polymerase:RNase H ratio can have profound effects on both polymerase and RNase H cleavage activities, as expected for an enzyme with two interdependent domains.

Reverse transcriptase (RT)[1] is a virion-associated enzyme encoded by the *pol* gene of all retroviruses, which catalyzes the synthesis of a double-stranded DNA copy of the viral RNA genome (Gilboa et al., 1979). The enzyme is multifunctional (Varmus & Swanstrom, 1984) and has several activities: RNA-dependent DNA polymerase activity; DNA-dependent DNA polymerase activity; and RNase H activity, which leads to degradation of the RNA moiety in an RNA·DNA hybrid (Moelling et al., 1971; Keller & Crouch, 1972; Leis et al., 1973). These activities reside on the same polypeptide (Baltimore & Smoler, 1972; Grandgenett et al., 1972; Keller & Crouch, 1972; Moelling, 1974; Verma, 1975), but the existence of independent active sites for the polymerase and RNase H functions was inferred from differential sensitivity to inhibitors (Brewer & Wells, 1974; Modak, 1976; Gorecki & Panet, 1978; Tan et al., 1991). Indeed, studies on MuLV and HIV RTs have shown that the polymerase and RNase H domains can be localized to the N- and C-terminal regions of the enzyme, respectively (Johnson et al., 1986; Hansen et al., 1988; Hizi et al., 1988; Kotewicz et al., 1988; Levin et al., 1988; Tanese & Goff, 1988; Prasad & Goff, 1989; Hizi et al., 1991). Evidence for the organization of RT into separate domains has also been obtained from recent work on the X-ray crystal structures of *Escherichia coli* RNase H (Katayanagi et al., 1990; Yang et al., 1990), HIV-1 RNase H (Davies et al., 1991), and HIV-1 RT (Arnold et al., 1992; Kohlstaedt et al., 1992).

In an earlier study (Levin et al., 1988), we pointed out that although the polymerase and RNase H activities of RT can each function in the absence of sequences from the other domain (Moelling, 1976; Lai & Verma, 1978; Gerard, 1981; Kotewicz et al., 1988; Levin et al., 1988; Tanese & Goff, 1988), under normal biological conditions there must be an interaction between the domains, which is required for proper folding of the enzyme and for complete transcription of the viral RNA genome during virus replication. The first attempt to conceptualize functional activity in terms of RT structure was made by Oyama et al. (1989). On the basis of that study, a model was proposed in which the position of the polymerase catalytic site is located at the 3′-terminus of the nascent DNA strand at a fixed distance from the RNase H active center; the model also envisioned tight coupling of polymerization

† This work was supported in part by the National Institutes of Health Intramural AIDS Targeted Antiviral Program.

* Corresponding author.

‡ National Institutes of Health.

§ Present address: Department of Pathology, Thomas Jefferson University, Philadelphia, Pennsylvania 19107.

‖ Mitsubishi Kasei Institute of Life Sciences.

[1] Abbreviations: RT, reverse transcriptase; MuLV, murine leukemia virus; HIV, human immunodeficiency virus; AMV, avian myeloblastosis virus; RAV-2, Rous-associated virus 2; nt, nucleotide(s); PMSF, phenylmethanesulfonyl fluoride; dNTPs, deoxyribonucleoside triphosphates; ddNTPs, 2′,3′-dideoxyribonucleoside triphosphates; kb, kilobases; bp, base pairs, LB broth, Luria–Bertani broth; SP, sulfonyl propionate; DTT, dithiothreitol; SDS, sodium dodecyl sulfate; kDa, kilodaltons.

0006-2960/93/0432-5508$04.00/0

and RNase H activities, with synthesis of a small amount of DNA followed by RNase H cleavage of the transcribed RNA. Experimentally, it has been shown that the RTs of MuLV, HIV, and the avian retroviruses AMV and RAV-2 exhibit RNase H cleavage patterns which are consistent with a fixed distance of 14–18 nucleotides between the two active sites (Oyama et al., 1989; Wohrl & Moelling, 1990; Luo & Taylor, 1990; Furfine & Reardon, 1991; Fu & Taylor, 1992; Gopalakrishnan et al., 1992). Although some evidence has been presented suggesting that the polymerase and RNase H activities are not strictly coupled (Huber et al., 1989; De Stefano et al., 1991a; Kati et al., 1992), other studies are, in general, in accord with the prediction made by the model (Oyama et al., 1989; Schatz et al., 1990; Wohrl & Moelling, 1990; Luo & Taylor, 1990; Furfine & Reardon, 1991; Fu & Taylor, 1992; Gopalakrishnan et al., 1992). The model has also received strong support from results describing the three-dimensional structure of HIV-1 RT (Arnold et al., 1992; Kohlstaedt et al., 1992).

The goal of the present study was to further evaluate the functional relationship between the polymerase and RNase H domains. We have performed detailed studies on wild-type MuLV RT, and we also describe an RT mutant which is missing the entire RNase H domain. In addition, we have examined the effects of unique alterations in the primary sequence of MuLV RT that (i) delete sequences in the region corresponding to the "connection" subdomain (Kohlstaedt et al., 1992) of HIV-1 RT and (ii) replace the MuLV RNase H domain with the complete sequence of *E. coli* RNase H (Kanaya & Crouch, 1983). The possibility that RT may have evolved by fusing a cellular RNase H with a retroviral polymerase (Oyama et al., 1989) led us initially to express the chimeric protein and to determine whether its RNase H activity would present a "viral" or a "cellular" phenotype.

Our results with wild-type RT are in agreement with the idea that the major RNase H cleavage event is coordinated with DNA synthesis. We present a model based on the structure of the enzyme to explain other cleavages which occur closer to the 5′-terminus of the RNA. We also show that mutations which most likely affect the spatial relationship between the two activities and the polymerase:RNase H ratio qualitatively and quantitatively affect polymerase activity and cleavage activity, as expected from the interdependence of the two RT domains.

MATERIALS AND METHODS

Materials. PMSF and the Micro BCA kit for determination of protein concentration were purchased from Pierce. [α-^{32}P]ATP (800 Ci/mmol) was obtained from New England Nuclear Corp. The HPLC columns were manufactured by TosoHaas and were purchased from Thomson Inc. Sephacryl S-200, dNTPs, ddNTPs, poly(rA)·oligo(dT), and poly(dT) were purchased from Pharmacia LKB Biotechnology Inc. DNA oligonucleotides were synthesized on a Biosearch Synthesizer Model 8750 (New Brunswick Scientific Co.). The Sequenase kit which contains single-stranded phage M13mp18 was purchased from U. S. Biochemical Corp.

Bacterial Strains and Plasmids. Derivation of the *lacZ*$^+$ parent clone, pRT24 (Hu et al., 1986), from the expression vector pWS50 (Sisk et al., 1986) has been described (Hu et al., 1986). Plasmid pRT24 contains sequences encoding the first 13 amino acids of the λ cII protein joined to the AKR MuLV RT coding region (minus the first 12 nt), 456 nt encoding the 5′ portion of integrase, and the coding region for *lacZ* (Hu et al., 1986). All plasmids were isolated in *E. coli* strain DC 519 (Hu et al. 1986; Sisk et al., 1986) and were transferred to *E. coli* strain DC520 (Hu et al., 1986; Sisk et al., 1986) for expression. In some cases, an RNase H-minus (*rnhA-339::cat*) version of DC520 was used; the mutation was introduced by P1 transduction from MIC3001 (Itaya & Crouch, 1991).

Construction of Plasmids. To prepare the wild-type RT clone, P_AH_A, plasmid pRT24 (Hu et al., 1986) was cut at two unique sites, *Xma*I [nt 4579, according to the numbering system of Herr (1984), near the 3′-end of the AKR MuLV RT coding region] and *Nhe*I [in the *lacZ* region of pWS50 (Sisk et al., 1986)]. The resulting large fragment (~9 kb) was ligated to a 62-bp double-stranded oligonucleotide whose coding strand contained the RT sequence from nt 4580 to 4625 (Herr, 1984) followed by a TAA termination codon in three reading frames, a *Hin*dIII site, and the 5′ G of the *Nhe*I site. Clone $pP(\Delta SX)_AH_A$ was generated by digesting pP_AH_A at unique *Sal*I (nt 3720) and *Xho*I (nt 4098) sites in the AKR MuLV RT coding region (Herr, 1984); the digested DNA was religated in a reaction containing a low DNA concentration (50 ng in a 20-μL final volume). Clone $pP_A\Delta H$ was constructed by digesting pRT24 (Hu et al., 1986) with *Xho*I and *Nhe*I. The resulting large fragment (~8.5 kb) was ligated to a 21-bp double-stranded oligonucleotide containing (in the coding strand) the sequence TCGAG from the *Xho*I site followed by a TAA termination codon in three frames, a *Hin*dIII site, and the 5′ G of the *Nhe*I site. To prepare the chimeric clone, pP_AH_{EC}, the large *Xho*I–*Nhe*I fragment of pRT24 (Hu et al., 1986) was ligated to another *Xho*I–*Nhe*I fragment obtained from plasmid pNT1 (E. Kalman and R. Crouch, unpublished data), which encodes the entire *E. coli* RNase H protein (Kanaya & Crouch, 1983). [pNT1 contains an *Xho*I site followed by an *Nde*I site, the ATG of which is the methionine codon initiating the *E. coli* RNase H protein (Kanaya & Crouch, 1983). The TAA termination codon for the RNase H protein (Kanaya & Crouch, 1983) is immediately followed by an *Nhe*I site.] For each of the clones, the inserts and surrounding regions were sequenced using a Sequenase kit. Like the protein expressed by the parent clone pRT24 (Hu et al., 1986), all of the proteins expressed by the new clones have the short N-terminal leader peptide joined to amino acid 5 of RT.

Enzyme Expression and Purification. To express the RT clones, 2 mL of LB broth containing 50 μg/mL ampicillin was inoculated with one colony and incubated at 32 °C. After 7 h, the entire 2-mL culture was added to 100 mL of LB broth containing 50 μg/mL ampicillin and incubated overnight at 32 °C. Forty milliliters of the overnight culture was transferred to 500 mL of LB broth containing 50 μg/mL ampicillin and incubated at 32 °C until the absorbance at 600 nm was 0.5–0.6. To induce expression of sequences under the control of the λ pL promoter, the culture was then shifted to 36 °C for 4 h. The cells were centrifuged in a Sorvall GS-3 rotor for 15 min at 2661*g*, washed one time with Tris-buffered saline, pH 7.4, placed on dry ice, and stored at −80 °C.

Soluble extracts were prepared from approximately 5 g of cell pellets (derived from 500-mL cultures) according to the procedure of Lautenberger et al. (1983), except that PMSF (1 mM final concentration) was added when the bacteria were disrupted. The final salt concentration of the extracts was 0.1 M. Following passage through 0.45-μm filters, extracts were loaded onto a DEAE-5PW column (150 × 21.5 mm) which was connected to a SP–5PW column (150 × 21.5 mm) at a flow rate of 2 mL per min; the DEAE column was washed with 0.1 M NaCl in modified buffer A (Levin et al., 1988)

containing 20% glycerol (instead of 5% glycerol). RT passes through the DEAE column and is bound to the SP column. RT was eluted from the SP column by using a linear gradient from 0.1 to 0.75 M NaCl in modified buffer A (Levin et al., 1988) at a flow rate of 2 mL per min. Fractions (2 mL) containing a protein with the appropriate molecular size (as determined by Coomassie blue staining of 10% SDS–polyacrylamide gels) and having either polymerase or RNase H activity or both (see below under Polymerase and RNase H Assays) were eluted at a salt concentration of 0.2–0.3 M NaCl. The peak fractions from the SP column were pooled and concentrated to a final volume of approximately 1 mL with the Centricon-30 filter system and were then loaded onto a Sephacryl S-200 column (1 × 120 cm). The Sephacryl column was equilibrated with 0.1 M NaCl in modified buffer A (Levin et al., 1988) and run at a rate of 5 mL per h using gravity (i.e., without a pump). One-milliliter fractions were collected and scanned for the presence of a protein of the expected molecular size (see above). The peak fractions were pooled, concentrated 5-fold with the Centricon-30 filter system, and then assayed for polymerase and RNase H activities. Several independent preparations of each RT were made, and in each case comparable results were obtained.

Polymerase and RNase H Assays. Polymerase activity was assayed with the synthetic primer/template, poly(rA)·oligo(dT), as described (Levin et al., 1974; Levin et al., 1988) except that $MnCl_2$ (final concentration, 0.5 mM) was used. One unit of polymerase activity is defined as 1 pmol of [^{3}H]dTMP incorporated in response to poly(rA)·oligo(dT) in 40 min at 37 °C (see Table I). Assay of RNase H activity with the homopolymeric substrate poly(rA)·poly(dT) was performed as described by Levin et al. (1988) with $MnCl_2$ (final concentration, 1 mM) or $MgCl_2$ (final concentration, 10 mM). The substrate was synthesized as described previously (Levin et al., 1988), except that the ATP was labeled with ^{32}P, and was purified as described by Hall and Crouch (1977). Units of RNase H activity refer to assay of RNase H with [^{32}P]poly(rA)·poly(dT) in reactions containing Mg^{2+} (see Table I); one unit is defined as degradation of 1 pmol of substrate in 15 min at 37 °C.

Uniformly labeled [^{32}P]RNA_{160} (a 160-nt ovalbumin RNA fragment) was prepared and purified as described by Oyama et al. (1989) except that [α-^{32}P]ATP was used to label the RNA. One picomole of the ^{32}P-labeled RNA (~50 000 cpm) was hybridized to 2 pmol of a 20-nt DNA oligonucleotide complementary to nt 3–22 upstream of the 3′-end of the RNA (Oyama et al., 1989) at 68 °C for 5 min in buffer containing 40 mM Tris-HCl, pH 7.5, 40 mM NaCl, and 5 mM $MgCl_2$. The hybrid was assayed in 10-μL reaction mixtures containing the same buffer as that used for the hybridization, 1 mM DTT, and RT, as indicated. In experiments in which cleavage was measured under conditions which permit extension of the DNA oligonucleotide primer, reactions also contained 0.125 mM each of 1 ddNTP and 3 dNTPs (ddNTP mixture). After incubation at 37 °C for 20 min, a 3-μL portion of the reaction mixture was added to 2 μL of RNA loading buffer (80% formamide, 50 mM Tris-borate, pH 8.2, 1 mM EDTA, 0.1% bromphenol blue, and 0.1% xylene cyanol); 3.5 μL of this mixture was run on a 6% sequencing gel.

Gel Renaturation Assay of RNase H Activity. Samples were electrophoresed in an SDS-polyacrylamide gel containing 2×10^7 cpm of ^{32}P-labeled poly(rA)·poly(dT) substrate (see above). After termination of the run, the gel was incubated for 4 days at room temperature in buffer containing 50 mM Tris-HCl, pH 8.0, 2 mM $MnCl_2$ or 10 mM $MgCl_2$ (as indicated), 5 mM DTT, and 50 mM NaCl, with several changes of buffer each day. The gel was exposed to XAR-5 film and subsequently stained with Coomassie blue. In this assay, degradation of the substrate is indicated by the presence of a clear band (at the position of the active protein) in the dark background of the autoradiogram. For ease of presentation, we have made a negative print; thus, bands corresponding to the active proteins are black and appear in a light background.

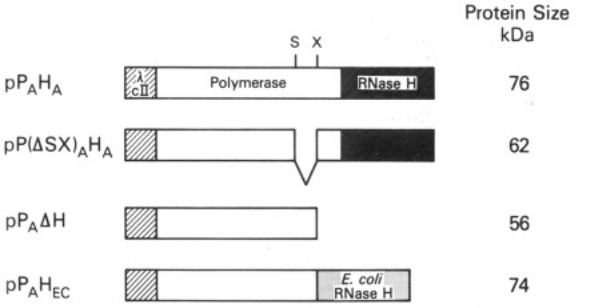

FIGURE 1: Schematic representation of insert sequences in AKR MuLV RT clones. Construction of the clones is described under Materials and Methods. The λ cII leader sequence, the insert sequences, and the sizes of the expressed proteins are shown for RT clones pP_AH_A, $pP(\Delta SX)_AH_A$, $pP_A\Delta H$, and pP_AH_{EC}. The figure is not drawn to scale. P, polymerase domain; H, RNase H domain; S, *Sal*I; X, *Xho*I. Subscripts: A, AKR MuLV; EC, *E. coli*.

RESULTS

Expression of MuLV RT Clones in E. coli. To gain a more precise understanding of the relationship between the polymerase and RNase H domains, wild-type and mutant AKR MuLV RT clones were constructed and expressed in *E. coli* under the control of the λ pL promoter (Figure 1). The wild-type clone, pP_AH_A, contains sequences encoding the polymerase and RNase H domains of AKR MuLV RT and expresses a 76-kDa protein. An RNase H-minus clone, $pP_A\Delta H$, contains polymerase sequences up to the *Xho*I site and expresses a 56-kDa RT missing the entire RNase H domain. Two other mutant clones include (i) pP_AH_{EC}, which contains AKR MuLV polymerase sequences up to the *Xho*I site fused to the entire coding region of *E. coli* RNase H (Kanaya & Crouch, 1983) and expresses a 74-kDa chimeric protein; and (ii) $pP(\Delta SX)_AH_A$, which is produced by an in-frame deletion of sequences between unique *Sal*I and *Xho*I sites (Herr, 1984) and expresses a 62-kDa RT missing 126 amino acids from the polymerase domain in a region immediately upstream of the RNase H domain. Johnson et al. (1986) suggested that this region may serve as a "tether" joining the two catalytic domains of RT. Comparison of the HIV-1 and MuLV RT sequences (Doolittle et al., 1989) taken in conjunction with recent information on the structural organization of HIV-1 RT (Kohlstaedt et al., 1992) suggests that this region in MuLV RT is analogous to the connection subdomain in the polymerase portion of the HIV-1 p66 subunit. The connection subdomain is adjacent to the RNase H domain in the primary sequence and also contacts the RNase H domain in the three-dimensional structure (Kohlstaedt et al., 1992).

In our initial studies, the RT proteins were expressed at 42 °C for 1 h; RNase H activity was tested by using a gel renaturation assay (see Materials and Methods). Figure 2, panel IA, shows the Coomassie blue-stained protein pattern, and panel IB, the RNase H activity, of the insoluble pellet fraction of three of the RT clones; the assay was performed in the presence of $MnCl_2$. In each case, several protein concentrations were tested. As may be seen, the extract from

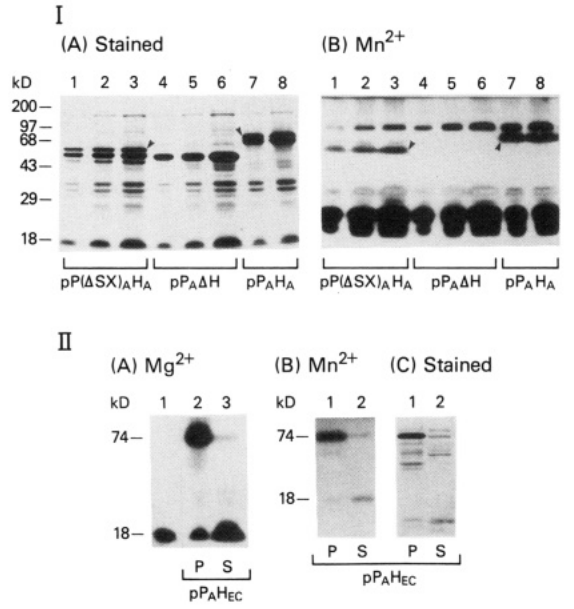

FIGURE 2: Gel assay of RNase H activity. Plasmids were expressed in 40-mL cultures at 42 °C for 1 h. Extracts were prepared according to Lautenberger et al. (1983), as described under Materials and Methods. The pellet fraction obtained after centrifugation of the lysate was resuspended directly in 0.25 mL of loading buffer (Hu et al., 1986). On the basis of the final absorbance at 600 nm of 1.3 for 1 mL of the 40-mL cultures, we calculate that 1 μL of this suspension was equivalent to the pellet fraction from 2×10^8 cells. The supernatant fraction was 1.2 mL; 1 μL was equivalent to the supernatant fraction from 0.42×10^8 cells. (I) Pellet fractions of clones $pP(\Delta SX)_AH_A$ (lanes 1–3), $pP_A\Delta H$ (lanes 4–6), and pP_AH_A (lanes 7 and 8) were electrophoresed in a 10% SDS–polyacrylamide gel. (IA) Coomassie blue stain. (IB) Activity assay with $MnCl_2$. The amounts added were as follows: lanes 1, 4, and 7, 5 μL; lanes 2, 5, and 8, 10 μL; lanes 3 and 6, 20 μL. (II) Pellet and supernatant fractions of clone pP_AH_{EC} were electrophoresed in a 12.5% SDS–polyacrylamide gel. (IIA) Activity assay with $MgCl_2$. Lane 1, purified *E. coli* RNase H (Kanaya & Crouch, 1983), 7 μg of protein; lane 2, pellet fraction; lane 3, supernatant fraction. (IIB) Activity assay with $MnCl_2$. Lane 1, pellet fraction; lane 2, supernatant fraction. (IIC) Coomassie blue stain of lanes 1 and 2 shown in (IIB). The amounts of pellet and supernatant fractions added were 10 and 25 μL, respectively. The molecular masses of the standard proteins are indicated on the left in panel IA. The proteins used were myosin (200 kDa), phosphorylase B (97 kDa), bovine serum albumin (68 kDa), ovalbumin (43 kDa), carbonic anhydrase (29 kDa), and β-lactoglobulin (18 kDa). The arrowheads in panels IA and IB denote the positions of proteins which exhibit activity in the RNase H assay. P, pellet fraction; S, supernatant fraction.

the wild-type clone, pP_AH_A, contained two major proteins: one, a 76-kDa band (denoted by an arrowhead) having the expected size of the full-length translation product, and the other, a smaller band at 69 kDa (IA, lanes 7 and 8). Only the larger band exhibited activity in this assay (IB, lanes 7 and 8). The 69-kDa protein is presumably the same protein as that observed earlier during expression of clone pRT250 (Levin et al., 1988) and is formed by C-terminal processing of the 76-kDa protein in *E. coli*. Thus, the 69-kDa protein reacts with a monoclonal antiserum directed against the N-terminal cII leader peptide (Levin et al., 1988) and a peptide antiserum directed against sequences in the N-terminal region of the RNase H domain, but not with a peptide antiserum directed against sequences at the C-terminus of RT (K. Post and J. G. Levin, unpublished data). These data support our earlier conclusion that the 69-kDa protein terminates within or near the amino acid sequence EGREIK and is missing sequences from the C-terminal half of the RNase H domain (Levin et al., 1988).

The results obtained with clone $pP(\Delta SX)_AH_A$ are illustrated in Figure 2, panels IA and IB, lanes 1–3. The 62-kDa primary translation product (denoted by an arrowhead) had RNase H activity (IB, lanes 1–3). The two smaller proteins migrating slightly faster than the 62-kDa protein (IA, lanes 1–3) did not have activity (IB, lanes 1–3) and are likely to be derived by proteolytic cleavage of the full-length product. As anticipated, no RNase H activity was associated with the major 56-kDa band or with smaller products expressed by clone $pP_A\Delta H$ (IA and IB, lanes 4–6).

The high molecular weight activity band seen in all lanes in panel IB at the position corresponding to a molecular weight of approximately 100 kDa is probably due to activity of the *E. coli* Pol I enzyme. The lower molecular weight bands, also seen in all lanes in panel IB, represent *E. coli* RNase H activity.

Analysis of clone pP_AH_{EC} is shown in Figure 2, panels IIA, IIB, and IIC. Because *E. coli* RNase H has activity in the presence of both Mg^{2+} and Mn^{2+}, the chimeric protein was assayed with $MgCl_2$ (IIA) and $MnCl_2$ (IIB). As shown in panel IIA, most of the activity associated with the 74-kDa translation product was in the pellet fraction (lane 2). In contrast, *E. coli* RNase H activity present in the extract was more prominent in the supernatant fraction (lane 3). The position of *E. coli* RNase H in the gel was verified by electrophoresis of purified enzyme (Kanaya & Crouch, 1983) (lane 1). The results obtained in the $MnCl_2$ assay (IIB) paralleled those with $MgCl_2$ (IIA), except that activity was higher in the presence of Mg^{2+}. Panel IIC shows lanes 1 and 2 of panel IIB after the proteins were stained with Coomassie blue; the 74-kDa protein was detected in both bacterial cell fractions. It should be noted that while *E. coli* RNase H in the supernatant fraction had significant activity (IIB, lane 2), it could not be visualized with the Coomassie stain (IIC, lane 2). This observation presumably reflects the high efficiency of renaturation of *E. coli* RNase H under the conditions of the assay.

The results of Figure 2 demonstrate that, for each RNase H-positive clone, RNase H activity was associated with an RT protein with the predicted molecular weight (Figure 1). In addition, the data show that, like *E. coli* RNase H, the chimeric protein expressed by clone pP_AH_{EC} has activity in the presence of Mg^{2+} and Mn^{2+} cations but clearly exhibits a preference for Mg^{2+}.

Purification and Specific Activities of MuLV RT Proteins. The results illustrated in Figure 2 indicated that in order to obtain purified proteins for detailed enzymatic studies, it would be important to find expression conditions which eliminate or at least minimize bacterial proteolysis within the RNase H domain and also lead to expression of large amounts of soluble protein. To address these problems, we expressed clone pP_AH_A at several temperatures for varying times and analyzed the proteins in the insoluble and supernatant fractions of the bacterial lysate (Lautenberger et al., 1983). At 36 °C, most of the RT in the supernatant fraction was present as the 76-kDa protein, and very little was present as the 69-kDa protein (data not shown). On the basis of these results, the RT clones were routinely expressed in all subsequent experiments at 36 °C for 4 h.

The RT proteins were purified from 500-mL cultures; the purification scheme is described in detail under Materials and Methods. Analysis of the purified proteins by SDS–PAGE and Coomassie blue staining is illustrated in Figure 3. The data in panel A indicate that while the soluble extracts of clones pP_AH_{EC} (lane 1) and pP_AH_A (lane 4) had a large number of proteins, the material from the SP column (lanes

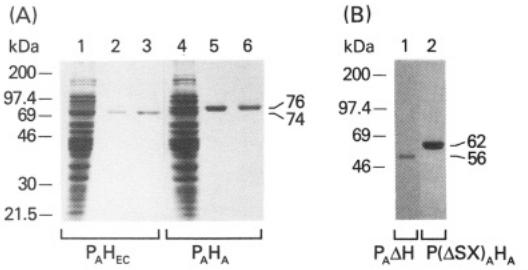

FIGURE 3: Gel analysis of purified AKR MuLV RT proteins. Proteins were electrophoresed in a 10% SDS–polyacrylamide gel and then stained with Coomassie blue. (A) Lane 1, P_AH_{EC}, soluble extract (200 μg of protein); lane 2, P_AH_{EC}, pooled fractions from the SP–5PW column (0.3 μg of protein); lane 3, P_AH_{EC}, pooled fractions from the Sephacryl S-200 column (0.6 μg of protein); lane 4, P_AH_A, soluble extract (200 μg of protein); lane 5, P_AH_A, pooled fractions from the SP–5PW column (7 μg of protein); lane 6, P_AH_A, pooled fractions from the Sephacryl S-200 column (5 μg of protein). (B) Lane 1, $P_A\Delta H$, pooled fractions from the Sephacryl S-200 column (0.5 μg of protein); lane 2, $P(\Delta SX)_AH_A$, pooled fractions from the Sephacryl S-200 column (3 μg of protein). The molecular masses of the standard proteins are shown on the left. The proteins used were myosin (200 kDa), phosphorylase B (97.4 kDa), bovine serum albumin (69 kDa), ovalbumin (46 kDa), carbonic anhydrase (30 kDa), and trypsin inhibitor (21.5 kDa). The molecular masses of the purified proteins are indicated on the right.

2 and 5) consisted almost entirely of the expressed 74- and 76-kDa RT proteins, respectively. At the final step of purification, one major band (lanes 3 and 6) was observed. Panel B shows that the final preparations of $P_A\Delta H$ (lane 1) and $P(\Delta SX)_AH_A$ (lane 2) contained the expected 56- and 62-kDa proteins (Figure 1), respectively. In the original gels it was also possible to visualize a few minor bands; each of the four enzyme preparations was therefore estimated to be 85–90% pure.

The purified RT proteins were further characterized by determining the specific polymerase and RNase H activities (Table I) in assays utilizing a homopolymeric primer/template [poly(rA)·oligo(dT)] or an RNA·DNA hybrid substrate [poly(rA)·poly(dT)], respectively, as described under Materials and Methods. RNase H activity was measured in reaction mixtures containing $MnCl_2$ or $MgCl_2$. The wild-type RT, P_AH_A, exhibited a high level of polymerase activity; the RNase H activity was also high, and as is characteristic for MuLV RT (Moelling, 1974; Verma, 1975), the enzyme showed a marked preference for Mn^{2+} compared with Mg^{2+} (35-fold). $P_A\Delta H$ had no detectable RNase H activity with either cation, but its specific activity value for polymerase was severalfold higher than wild type. A similar observation has been made for other MuLV RTs which are missing the RNase H domain (Hizi et al., 1990; Telesnitsky et al., 1992). The deletion mutant, $P(\Delta SX)_AH_A$, had essentially no polymerase activity and also exhibited a significant reduction in RNase H activity in the presence of Mg^{2+}. P_AH_{EC} had the same specific polymerase activity as the wild type in the poly(rA)·oligo(dT) assay, but its RNase H activity was like that of purified *E. coli* RNase H (Kanaya & Crouch, 1983), with respect to both metal ion preference and high specific activity.

The analysis of the purified P_AH_A, $P(\Delta SX)_AH_A$, and $P_A\Delta H$ RTs showing very low (or no) RNase H activity in the presence of Mg^{2+} indicates that these enzyme preparations were not contaminated with *E. coli* RNase H. In the case of P_AH_{EC}, this cannot be evaluated directly, but it should be noted that the RNase H activity of enzyme purified from an RNase H-minus strain of *E. coli* (see Materials and Methods) was the same as that shown in Table I (data not shown). Polymerase activity was also assayed in response to poly(dA)·oligo(dT); the specific activity was generally less than or equal to 1 pmol/μg of protein (data not shown), indicating that there was little or no contamination with *E. coli* Pol I.

Table I: Polymerase and RNase H Activities of RT Proteins

RT protein	polymerase[a]	RNase H[b]	
		Mn^{2+}	Mg^{2+}
	pmol incorpd/μg of protein	pmol degraded/μg of protein	
P_AH_A	21 000	840	24
$P_A\Delta H$	49 000	<0.2	<0.2
$P(\Delta SX)_AH_A$	2.5	424	1.0
P_AH_{EC}	22 000	1740	250 000

[a] Polymerase activity is measured as pmol of [^{3}H]dTMP incorporated in response to poly(rA)·oligo(dT). [b] RNase H activity is measured as pmol of [^{32}P]poly(rA)·poly(dT) degraded.

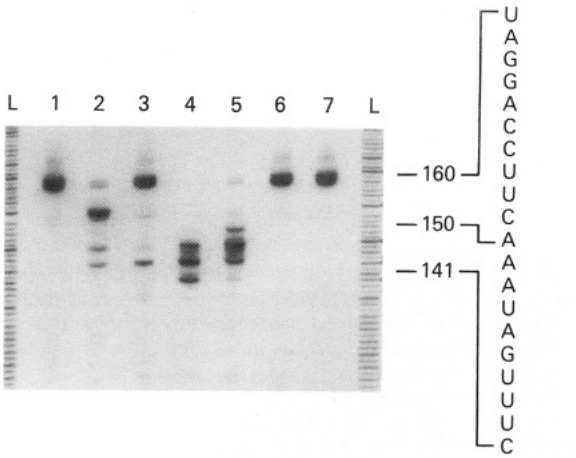

FIGURE 4: RNase H digestion products obtained with a substrate containing ^{32}P-labeled RNA_{160} hybridized to a 20-nt DNA oligonucleotide. The hybridization conditions, the assay of RNase H activity, and the definition of RNase H units (H) are given under Materials and Methods. The sizes of RNA fragments generated by RNase H cleavage were estimated by comparison with a coelectrophoresed DNA sequencing ladder; the estimates were based on the assumption that the position of RNA_{160} indicates nt 160 (Oyama et al., 1989). The nucleotide sequence of the ovalbumin RNA fragment at positions 141–160 is shown on the right. Lane 1, no enzyme; lane 2, P_AH_A, 0.12 unit (H), 4.8 ng of protein; lane 3, $P(\Delta SX)_AH_A$, 0.18 unit (H), 0.18 μg of protein; lane 4, P_AH_{EC}, 113 units (H), 0.45 ng of protein; lane 5, *E. coli* RNase H, 15 units (H), 0.2 ng of protein; lane 6, $P_A\Delta H$, 4.4 ng of protein; lane 7, no enzyme. The particular *E. coli* RNase H preparation used in this experiment had a specific activity about 2-fold lower than normal (Kanaya & Crouch, 1983; data not shown). The lanes labeled L are sequencing ladders made by mixing the A, C, T, and G sequencing reactions of M13mp18.

RNase H Cleavage Products Generated from a Complex RNA·DNA Hybrid Substrate without Concurrent DNA Synthesis. It was of interest to characterize the RNase H activity of the purified RTs with a substrate more complex than poly(rA)·poly(dT). For this work, we chose the heteropolymeric substrate used in the earlier study by Oyama et al. (1989); this substrate consists of a 160-nt ovalbumin RNA fragment (RNA_{160}) hybridized to a 20-nt complementary DNA oligonucleotide at a site located 2 nt from the 3′-end of the RNA. Gel analysis of the cleavage products obtained in the absence of polymerization is shown in Figure 4. Cleavage catalyzed by the wild-type enzyme (lane 2) occurred at positions corresponding to 15, 9, and 6 nt from the 3′-end of the DNA oligonucleotide (153-, 147-, and 144-nt products, respectively), but the 153-nt fragment represented the major cleavage product. There was also a very weak band corresponding to a 150-nt product. At a limiting concentration of enzyme, the only cleavage product detected was the 153-nt

fragment (data not shown). In contrast, at high enzyme concentrations, cleavages closer to the 5′-end of the RNA (i.e., closer to the 3′-end of the DNA) were more prominent and, indeed, the 153-nt product was not seen when excess MuLV RT was used (Oyama et al., 1989). Presumably, when the 160-nt RNA is shortened to 153 nt, the resulting hybrid is a poor substrate at low concentrations of RT; however, when more RT is present, additional cleavage occurs.

Large amounts of enzyme were needed to obtain cleavage with $P(\Delta SX)_AH_A$ (Figure 4, lane 3); the most prominent cleavage product occurred at a position corresponding to 6 nt from the 3′-end of the DNA oligonucleotide (144-nt product), although trace amounts of the 153- and 147-nt products were also observed. The cleavage products generated by P_AH_{EC} (lane 4) were numerous and, in general, shorter than those obtained with wild-type RT; the most prominent bands occurred at positions 6, 9, and 3 nt from the 3′-end of the DNA oligonucleotide (144-, 147-, and 141-nt products, respectively). The pattern obtained with *E. coli* RNase H (lane 5) was similar to that of P_AH_{EC}, except that the band corresponding to the 141-nt product was very weak and there was a band of moderate intensity at a position 12 nt from the 3′-end of the DNA (150-nt product), which was very faint in the P_AH_{EC} pattern. The differences in the P_AH_{EC} and *E. coli* RNase H patterns are due to the fact that the P_AH_{EC} reaction mixtures contained more units of RNase H activity than those with *E. coli* RNase H. Thus, when a lower concentration of P_AH_{EC} was used and some of the RNA_{160} remained undigested, the 150-nt product was more readily detected and the 141-nt product was less prominent (data not shown). As expected, $P_A\Delta H$ (lane 6) did not exhibit any RNase H activity.

Analysis of Polymerase Activity under Conditions of Limited Primer Extension. It is clearly important to evaluate RNase H activity under conditions where DNA synthesis is also occurring. Since this study involves mutant and wild-type enzymes, initial experiments were performed to examine polymerization with the RNA_{160} template. Reactions were carried out in the presence of unlabeled RNA_{160}, ^{32}P-5′-end-labeled 20-nt primer, 3 dNTPs, and 1 ddNTP (Figure 5); in this situation, the ddNTP acts as a chain terminator of DNA synthesis and blocks further extension of the primer at the growing end of the DNA strand. Thus, with ddATP, ddCTP, ddTTP, and ddGTP, polymerization is terminated after extension by 1, 3, 8, and 18 nt, respectively (Oyama et al., 1989).

Figure 5A, lanes 1–5, shows the analysis of the wild-type reactions. Products corresponding to the predicted extensions of +3, +8, and +18 were observed in reactions with ddCTP (lane 3), ddTTP (lane 4), and ddGTP (lane 5), respectively. In each case, some smaller products were also observed and were presumably the result of pausing or premature termination of DNA synthesis. The presence of some 19-mer in the 20-nt primer preparation [note the band immediately below the unextended primer (labeled 0)] may account for products corresponding to extensions of +7 and +17 in the ddTTP (lane 4) and ddGTP (lane 5) reactions, respectively. Reactions with ddCTP (lane 3) and ddGTP (lane 5) also contained minor amounts of products which were slightly longer than expected; the explanation for this is unclear. With ddATP (lane 2), the predicted extension product of +1 could not be detected.

In contrast to the results obtained with the wild type, analysis of reactions containing the chimeric RT (Figure 5A, lanes 6–10) indicated that the predicted extension products were not detected in any of the reactions, even though the concentration of enzyme was increased 10-fold over that used

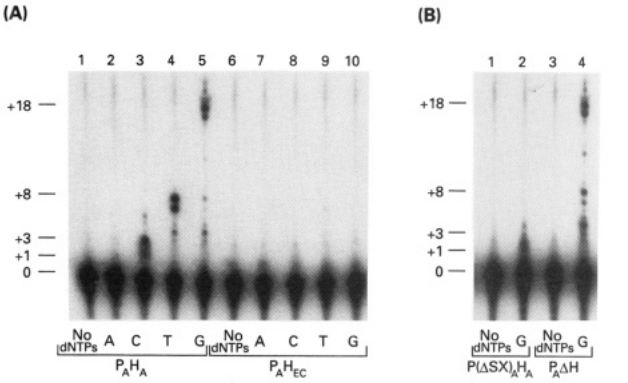

FIGURE 5: Limited extension of ^{32}P-labeled 20-nt DNA oligonucleotide primer with RNA_{160} as template. Unlabeled RNA_{160} (1 pmol) was hybridized to ^{32}P-5′-end-labeled 20-nt DNA primer (130 000 cpm, 0.07 pmol) and then incubated with RT and a mixture of 1 ddNTP and 3 dNTPs, as indicated. The conditions for primer extension with 1 ddNTP and 3 dNTPs and the definitions of polymerase (P) and RNase H (H) units, respectively, are given under Materials and Methods. After incubation, reactions were terminated by addition of 4 μL of STOP solution from a U.S. Biochemical Corp. Sequenase kit, and a 3.5-μL portion was run on a 8% sequencing gel. (A) Enzymes and amounts added were as follows: P_AH_A, 100 units (P), 0.12 unit (H), 4.8 ng of protein (lanes 1–5); P_AH_{EC}, 100 units (P), 1130 units (H), 4.5 ng of protein (lanes 6–10). Lanes 1 and 6, no dNTPs; lanes 2 and 7, ddATP mixture; lanes 3 and 8, ddCTP mixture; lanes 4 and 9, ddTTP mixture; lanes 5 and 10, ddGTP mixture. (B) Amounts of enzyme added were as follows: $P(\Delta SX)_AH_A$, 0.45 unit (P), 0.18 unit (H), 0.18 μg of protein (lanes 1 and 2); $P_A\Delta H$, 216 units (P), 4.4 ng of protein (lanes 3 and 4). Lanes 1 and 3, no dNTPs; lanes 2 and 4, ddGTP mixture. A, C, T, and G refer to reactions with 3 dNTPs and ddATP, ddCTP, ddTTP, or ddGTP, respectively. The numbers on the left side of each panel indicate the positions of DNA extensions of +1, +3, +8, and +18 which are predicted for reactions containing ddATP, ddCTP, ddTTP, and ddGTP, respectively; 0 refers to the unextended primer. A radioactive band immediately below the unextended primer represents a small amount of a 19-nt oligonucleotide in the 20-nt primer preparation. Since the oligonucleotides are synthesized in a 3′ → 5′ direction, the 19-mer should only be missing the final 5′ nucleotide (dC) (Oyama et al., 1989), present in the 20-nt primer.

in the experiment shown in Figure 4. In the presence of ddATP (lane 7) and ddCTP (lane 8), no extension was observed. With ddTTP (lane 9) and ddGTP (lane 10), some extension occurred, and in the case of ddTTP there was a small amount of a +7 extension product.

With $P(\Delta SX)_AH_A$ (Figure 5B, lanes 1 and 2), very little extension was observed in reactions with ddGTP (lane 2); small amounts of +3 and +4 extension products were detected, as well as traces of products up to an extension size of +10. This result was not surprising since $P(\Delta SX)_AH_A$ had virtually no polymerase activity in the polyrA·oligo dT assay (Table I). With $P_A\Delta H$ (Figure 5B, lanes 3 and 4), addition of ddGTP (lane 4) resulted in a distribution of products which was similar to that seen with the wild-type RT (Figure 5A, lane 5); in this case, however, there were relatively higher amounts of less than full length products. In addition, there were equivalent amounts of the +17 and +18 extension products, whereas in the wild-type reactions the +18 product was the major DNA synthesized. This result indicates that the RNase H-minus RT is less processive than the wild-type enzyme and is in accord with other experiments in which primer extension was measured on viral RNA and DNA templates in the presence of all four dNTPs (J. Guo, K. Post, R. J. Crouch, and J. G. Levin, unpublished data).

RNase H Cleavage Products Generated from the RNA_{160} Substrate with Concurrent DNA Synthesis. To determine the effect of dNTP addition on RNase H cleavage, reactions

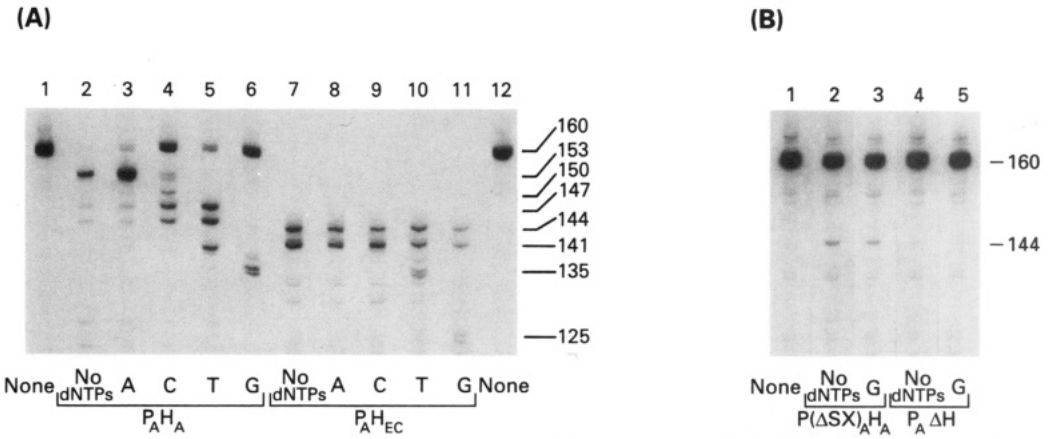

FIGURE 6: RNase H digestion products generated from the RNA_{160} substrate after incubation with P_AH_A, P_AH_{EC}, $P(\Delta SX)_AH_A$, and $P_A\Delta H$ RTs under conditions of limited primer extension. The assay conditions and amounts of enzyme were the same as those used to study polymerization and are given in the caption to Figure 5. The ^{32}P-labeled substrate was the same as that used in the experiment described in Figure 4. (A) Enzymes added were P_AH_A (lanes 2–6) and P_AH_{EC} (lanes 7–11). Lanes 1 and 12, no enzyme and no dNTPs; lanes 2 and 7, no dNTPs; lanes 3 and 8, ddATP mixture; lanes 4 and 9, ddCTP mixture; lanes 5 and 10, ddTTP mixture; lanes 6 and 11, ddGTP mixture. (B) Enzymes added were $P(\Delta SX)_AH_A$ (lanes 2 and 3) and $P_A\Delta H$ (lanes 4 and 5). Lane 1, no enzyme and no dNTPs; lanes 2 and 4, no dNTPs; lanes 3 and 5, ddGTP mixture. The nucleotide sizes of the individual cleavage products are indicated by the numbers on the right of each panel. None refers to reactions without enzyme and dNTPs; A, C, T, and G refer to reactions containing 3 dNTPs and ddATP, ddCTP, ddTTP, or ddGTP, respectively.

were performed under the same conditions as those used to study polymerization (see caption to Figure 5), except that ^{32}P-labeled RNA_{160} and unlabeled 20-nt primer were added (Figure 6). With the wild-type RT (Figure 6A, lanes 2–6), no change in the cleavage pattern could be detected in reactions with ddATP (compare lanes 3 and 2). This finding parallels the observation that, with ddATP, the predicted +1 extension product also could not be detected (Figure 5A, lane 2). In reactions with ddCTP (+3 extension), there was a decrease in the 153-nt product and a substantial increase in a 150-nt product (compare lanes 4 and 2); in addition, there was an increase in the 147- and 144-nt products. As shown in lane 5, addition of ddTTP (+8 extension) resulted in the loss of the 153-nt product and increased amounts of the 144- and 147-nt products. An additional 138-nt product was also seen. With ddGTP (+18 extension), the major cleavage products were 135 and 134 nt in length (lane 6). There were also minor amounts of larger products.

These results demonstrate that, in general, with a limiting concentration of the wild-type RT, as the DNA was extended, the RNA was correspondingly shortened; cleavage was detected at a position 14 or 15 nt from the 3′-end of the growing DNA chain. The exact position also appeared to depend on the local RNA sequence, and with the exception of the 150-nt product, it occurred between a 5′ U and the adjacent nucleotide [see the sequence of RNA_{160} in Oyama et al. (1989) and Figure 4].

Addition of dNTPs had no effect on the cleavage pattern obtained when P_AH_{EC} was present at the same concentration as that used in the experiment shown in Figure 4 (data not shown). When the concentration of enzyme was increased 10-fold, the products obtained in reaction mixtures containing 3 dNTPs and 1 ddNTP (Figure 6A, lanes 8–11) were similar, but not identical, to those obtained in the absence of triphosphates (Figure 6A, lane 7). Small amounts of new cleavage products were observed in the presence of ddTTP (lane 10) and ddGTP (lane 11), indicating that some extension had taken place in these reactions; however, the amounts of these new products were very low. These observations are in accord with the findings of Figure 5, demonstrating that the chimeric RT is deficient in its ability to synthesize DNA under the conditions of this assay.

No change in the cleavage pattern could be detected when a mixture containing ddGTP was added to reaction mixtures containing $P(\Delta SX)_AH_A$; in both the absence and the presence of dNTPs, one major band corresponding to the 144-nt product was observed (Figure 6B; compare lanes 2 and 3). This result is consistent with the finding that, under the conditions of this experiment, $P(\Delta SX)_AH_A$ synthesized only low amounts of small extension products (Figure 5B, lane 2). With $P_A\Delta H$, no RNase H activity was observed, either in the presence or in the absence of the ddGTP mixture (Figure 6B; compare lanes 4 and 5).

DISCUSSION

In the present study, we have investigated the functional relationship between the polymerase and RNase H domains of MuLV RT. RNase H activity was examined in detail, in both the absence and the presence of concurrent DNA synthesis, using the previously characterized RNA_{160} substrate (Oyama et al., 1989). We describe an RT, $P_A\Delta H$, which is missing the entire RNase H domain, as well as two other novel mutants: (i) a chimeric RT, P_AH_{EC}, in which the MuLV RNase H domain is replaced by *E. coli* RNase H, and (ii) $P(\Delta SX)_AH_A$, which has a 126 amino acid deletion in a region corresponding to the connection subdomain in the p66 subunit of HIV-1 RT (Kohlstaedt et al., 1992). Our data show that each of these mutations, while occurring in only one domain, results in an abnormal polymerase:RNase H ratio and has profound effects on both polymerase and RNase H cleavage activities.

The interpretation of the data is aided by recent studies on the three-dimensional structure of HIV-1 RT (Arnold et al., 1992; Kohlstaedt et al., 1992). HIV-1 and MuLV RTs share many properties, except that the HIV enzyme is active only in dimeric form (Jacobo-Molina & Arnold, 1991), while MuLV RT appears to be a monomer (Varmus & Swanstrom, 1984). For example, since $P(\Delta SX)_AH_A$ is missing most of the region which in HIV-1 RT contacts portions of the polymerase domain as well as the RNase H domain (Kohlstaedt et al., 1992), the mutation alters the spatial relationship between the two domains and the protein functions as if the domains are no longer interconnected. Not surprisingly, the

deletion leads to a large reduction in polymerase activity (Table I; Figure 5) and a significant decrease in RNase H activity (Table I). Results obtained with the RNA_{160} substrate demonstrate that both the quality and the quantity of RNase H cleavage by $P(\Delta SX)_AH_A$ differ from those seen with wild type (Figure 4); moreover, the cleavages are not affected by the inclusion of dNTPs in the reaction mixture (Figure 6). Curiously, one result of the mutation is a more dramatic effect on RNase H activity in the presence of Mg^{2+} compared with Mn^{2+} (Table I). In HIV, the isolated RNase H domain (expressed in *E. coli*) has no RNase H activity (Becerra et al., 1990; Hostomsky et al., 1991; Restle et al., 1991). It is of interest that this lack of activity is thought to result, at least in part (Kohlstaedt et al., 1992), from the fact that the His^{539}-containing loop which is located close to the two divalent metal ions at the RNase H catalytic center of HIV-1 RT is disordered in the isolated RNase H domain (Davies et al., 1991) and ordered in p66/51 RT (Kohlstaedt et al., 1992). This feature is the only major difference between the two three-dimensional structures (Davies et al., 1991; Arnold et al., 1992; Kohlstaedt et al., 1992).

The chimeric RT behaves like purified *E. coli* RNase H (Kanaya & Crouch, 1983) in assays with the homopolymeric (Table I) and RNA_{160} substrates (Figure 4), and unlike wild-type MuLV RT (Moelling, 1974; Verma, 1975; Table I), it exhibits a strong preference for Mg^{2+} over Mn^{2+} (Figure 2; Table I). Interestingly, in calculating the ratio of RNase H activity to polymerase activity using RNase H values from Table I obtained under optimal RNase H assay conditions (i.e., Mg^{2+} for P_AH_{EC} and Mn^{2+} for P_AH_A), we find that this ratio is much higher for P_AH_{EC} (11:1 ratio) than it is for the wild-type enzyme (1:25 ratio). These results demonstrate that fusion of the cellular RNase H with the viral polymerase produces an aberrant RT in which RNase H is the dominant activity.

The P_AH_{EC} cleavage pattern with the RNA_{160} substrate shows little or no change when dNTPs are present in the reaction mixture (Figure 6), reflecting the limited ability of this enzyme to carry out primer extension (Figure 5). Since the RNA_{160} assay is performed under conditions where the RNase H activity of the enzyme is very potent [i.e., in the presence of Mg^{2+} (Table I)], there may be substantial degradation of the RNA in the RNA·DNA hybrid before significant copying of the template can occur. The high level of polymerase activity seen in the Mn^{2+}-dependent assay with poly(rA)·oligo(dT) is possible because the RNase H activity of the chimeric RT with this cation is comparable to that of wild-type RT and approximately 150-fold lower than with Mg^{2+} (Table I). Similarly, it can be argued that the complete lack of RNase H activity in the $P_A\Delta H$ RT (Table I; Figures 4 and 6) accounts for the observation that this enzyme has a higher polymerase specific activity than the wild type (Table I).

Analysis of the wild-type RT with the RNA_{160} substrate reveals that the major cleavage product represents a cut in the RNA corresponding to a position 15 nt from the 3′-end of the 20-nt DNA primer (Figure 4), in accord with other studies (Oyama et al., 1989; Luo & Taylor, 1990; Wohrl & Moelling, 1990; Furfine & Reardon, 1991; Fu & Taylor, 1992; Gopalakrishnan et al., 1992; J. Guo, K. Post, R. J. Crouch, and J. G. Levin, unpublished data). These findings, as well as recent X-ray crystallographic studies on HIV-1 RT (Arnold et al., 1992; Kohlstaedt et al., 1992), support the proposal (Oyama et al., 1989) that recognition of the 3′-terminal OH of the DNA orients the RT protein and places the RNase H catalytic site at a fixed distance, i.e., 14–18 nt, from the 3′-OH position. Furthermore, evidence presented in this (Figures 5 and 6) and other reports (Oyama et al., 1989; Schatz et al., 1990; Wohrl & Moelling, 1990; Luo & Taylor, 1990; Furfine & Reardon, 1991; Gopalakrishnan et al., 1992) indicates that in general, when polymerization occurs, the major RNase H cleavage is coordinated with DNA synthesis. As noted above, cleavage is also influenced by local sequence (Figure 6; Oyama et al., 1989; Furfine & Reardon, 1991).

It is interesting that with the RNA_{160} substrate and wild-type RT significant amounts of RNA_{160} remain in reactions containing dNTPs (Figure 6A, lanes 3–6), but at the same enzyme concentration virtually all of the RNA is degraded in the absence of dNTPs (Figure 6A, lane 2). This suggests that once DNA synthesis begins, the enzyme may be bound to the two catalytic sites and no longer free to attack another molecule of RNA_{160}. Furfine and Reardon (1991) have made a similar observation with HIV-1 RT and have argued that after incorporation of a dideoxynucleotide, the presence of the next encoded dNTP may inhibit dissociation of the template·primer from RT.

In addition to the major RNase H cleavage site, we find, in agreement with others (Wohrl & Moelling, 1990; Schatz et al., 1990; Furfine & Reardon, 1991; De Stefano et al., 1991b; Wohrl et al., 1991; Gopalakrishnan et al., 1992), that sites close to the 3′-OH of the DNA can also be cleaved. With wild-type RT, these sites are detected mainly when an excess of enzyme is used (Figure 4; Oyama et al., 1989). Cleavage at the secondary sites can occur in the presence or absence of dNTPs (Figure 6) and is not coupled to DNA extension (Figure 6; Furfine & Reardon, 1991; Gopalakrishnan et al., 1992). Presumably, these sites have sequences which favor cleavage. Thus, the 144- and 147-nt secondary products produced in the absence of dNTPs (Figure 6A, lane 2) are also the major cleavage products formed during extension of +8 nucleotides with ddTTP (Figure 6A, lane 5), instead of an expected 145-nt product.

It is quite striking that, in contrast to wild-type RT, cleavages made by the mutant enzymes, P_AH_{EC} and $P(\Delta SX)_AH_A$, occur exclusively at secondary cleavage sites and are not coordinated with DNA synthesis (Figure 6). Thus, when the RNase H of *E. coli* is fused to the polymerase domain of MuLV, the polymerase domain has no influence on the cleavage pattern seen with the RNA_{160} substrate (Figure 6). Similarly, with $P(\Delta SX)_AH_A$, the 144- and 147-nt cleavage products are identical to the secondary products seen with the wild-type enzyme (Figure 6), and as discussed above, the RNase H activity of $P(\Delta SX)_AH_A$ functions independently of polymerase. These observations led to the conclusion that, for both mutants, binding of the RNA·DNA hybrid must be independent of the polymerase domain.

The secondary cleavages of the wild-type enzyme as well as the similar mutant cleavages appear to result from a primary interaction of the RNase H region of the enzyme with the RNA·DNA hybrid, in a manner which is also independent of the 3′-OH of the DNA component. We term such cleavages "3′-OH-independent".[2] That 3′-OH-independent cleavages can indeed occur is perhaps best illustrated by the ability of HIV-1 RT to cleave an RNA·DNA hybrid that is completely devoid of 3′-termini (Krug & Berger, 1989).

[2] "3′-OH-independent" is analogous to the term "polymerase-independent" (Furfine & Reardon, 1991; Peliska & Benkovic, 1992), but is more precise since for some RTs, e.g., HIV RT (Hostomsky et al., 1991), the polymerase domain is necessary for RNase H activity. "3′-OH" refers to the 3′-terminus of the DNA, even if extension of the DNA is terminated with a ddNTP.

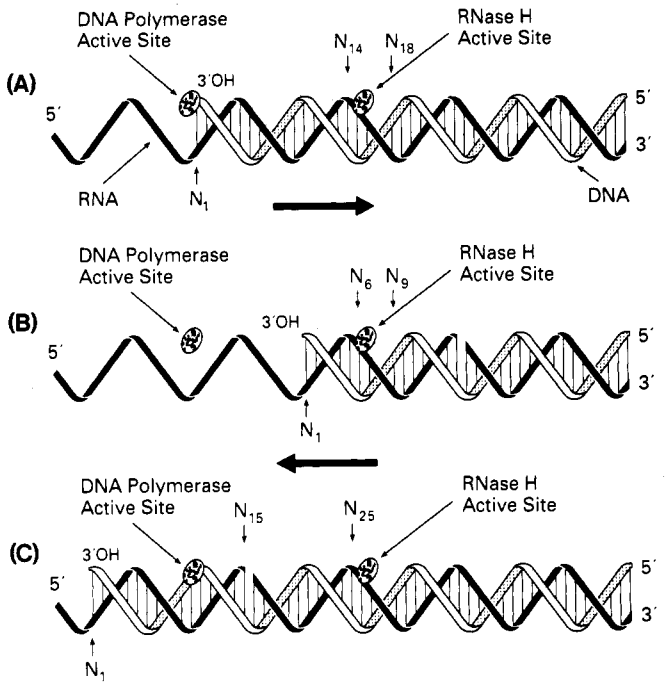

FIGURE 7: Scheme for 3′-OH-dependent and -independent cleavages of an RNA·DNA hybrid bound to RT. The DNA polymerase and RNase H active sites of RT are indicated on the figure. Nucleotide positions on the RNA are numbered with respect to the distance of a complementary deoxyribonucleotide from the 3′-OH of the DNA; e.g., N1 refers to the nucleotide which is complementary to the terminal deoxyribonucleotide at the 3′-OH. (A) 3′-OH-dependent cleavage. The 3′-OH of the DNA is shown bound to the polymerase active site. The polymerase and RNase H active sites are separated by a distance of 14–18 nt, and cleavage will occur at the position where the hybrid interacts with the RNase H site. (B) 3′-OH-independent cleavage. After the cleavage shown in (A), the hybrid is repositioned, as indicated by the solid arrow between (A) and (B), in a 3′ → 5′ direction (referring to the RNA strand) with respect to RT; the 3′-OH is no longer bound to the polymerase active site. Cleavages can now occur at nucleotides which are closer to the 3′-OH of the DNA. (C) Alternative 3′-OH-independent cleavage. The RNA·DNA hybrid is repositioned in a 5′ → 3′ direction (RNA strand), as indicated by the solid arrow between (B) and (C), with respect to RT. The 3′-OH of the DNA is always at a position which is away from the polymerase active site.

How can we explain 3′-OH-independent cleavages with more conventional substrates? In Figure 7, we present a general scheme relating binding of the RNA·DNA hybrid to the wild-type enzyme and the type of cleavage event; the scheme is based on our results with the RNA_{160} substrate, although the substrate shown represents a generic RNA·DNA hybrid. With wild-type RT, the major cleavage event, which is 3′-OH-dependent (Figure 7A), occurs 14–18 nucleotides from the 3′-OH of the DNA. (These nucleotide positions are designated N14–N18, where N1 is the nucleotide in the RNA which is complementary to the deoxyribonucleotide at the 3′-OH of the DNA.) After this cleavage (Figure 7B), the RNA·DNA hybrid is repositioned with respect to the enzyme and new cleavages take place at positions closer to the 3′-OH, e.g., at N6 and N9 (corresponding to the cuts generating the 144- and 147-nt products seen with the RNA_{160} substrate); in this case, the 3′-OH is no longer bound to the polymerase active site. In HIV-1 RT, the RNA·DNA hybrid fits in a groove connecting the polymerase and RNase H active sites (Kohlstaedt et al., 1992). Assuming that MuLV RT has a structure similar to that of HIV-1 RT, it seems likely that this groove would tend to keep the substrate from being completely released and could also aid in repositioning the hybrid on the enzyme.

The movement of the substrate shown in Figure 7B, i.e., in a 3′ → 5′ direction (referring to the RNA strand), has been observed previously (Schatz et al., 1990; DeStefano et al., 1991b; Wohrl et al., 1991) and may be necessary for DNA strand transfer (Peliska & Benkovic, 1992). In Figure 7C we have considered the theoretical possibility that the substrate moves in the other direction. As may be seen, were the RNA·DNA hybrid to move in this way, the polymerase active site would have no 3′-OH with which to interact. Fu and Taylor (1992) have described a two-step reaction in which DNA synthesis is uncoupled from cleavage; the DNA product is synthesized with an RNase H-minus RT and extends to the end of the RNA template; the resulting hybrid is then cleaved with an RNase H-plus enzyme. The 5′-cleavage product from this reaction is 14–18 nt in length and is presumably generated by the mechanism shown in Figure 7A. However, cleavage of the rest of the RNA could conceivably occur by the mechanism shown in Figure 7C. In a model in which DNA synthesis and RNA cleavage are uncoupled or in the case of the RNase H-minus RT product of Fu and Taylor (1992), for any cleavages other than the one related to the 3′-OH, the enzyme must find the RNA·DNA again, either by binding internally or by some processive mechanism. In either case, all of these cleavages would have to be 3′-OH-independent.

NOTE ADDED IN PROOF

After submission of this manuscript, a paper appeared which suggests that MuLV RT binds primer/template as a dimer, although the enzyme is monomeric in solution (Telesnitsky & Goff, 1993).

ACKNOWLEDGMENT

We thank Lisa Ng for outstanding technical assistance and Kathleen Shoobridge for expert help with preparation of the manuscript.

REFERENCES

Arnold, E., Jacobo-Molina, A., Nanni, R. G., Williams, R. L., Lu, X., Ding, J., Clark, A. D., Jr., Zhang, A., Ferris, A. L., Clark, P., Hizi, A., & Hughes, S. H. (1992) *Nature (London) 357*, 85–89.

Baltimore, D., & Smoler, D. F. (1972) *J. Biol. Chem. 247*, 7282–7287.

Becerra, S. P., Clore, G. M., Gronenborn, A. M., Karlstrom, A. R., Stahl, S. J., Wilson, S. H., & Wingfield, P. T. (1990) *FEBS Lett. 270*, 76–80.

Brewer, L. C., & Wells, R. D. (1974) *J. Virol. 14*, 1494–1502.

Davies, J. F., II, Hostomska, Z., Hostomsky, Z., Jordan, S. R., & Matthews, D. A. (1991) *Science 252*, 88–95.

DeStefano, J. J., Buiser, R. G., Mallaber, L. M., Myers, T. W., Bambara, R. A., & Fay, P. J. (1991a) *J. Biol. Chem. 266*, 7423–7431.

DeStefano, J. J., Buiser, R. G., Mallaber, L. M., Bambara, R. A., & Fay, P. J. (1991b) *J. Biol. Chem. 266*, 24295–24301.

Doolittle, R. F., Feng, D.-F., Johnson, M. S., & McClure, M. A. (1989) *Q. Rev. Biol. 64*, 1–30.

Fu, T.-B., & Taylor, J. (1992) *J. Virol. 66*, 4271–4278.

Furfine, E. S., & Reardon, J. E. (1991) *J. Biol. Chem. 266*, 406–412.

Gerard, G. F. (1981) *J. Virol. 37*, 748–754.

Gilboa, E., Mitra, S. W., Goff, S., & Baltimore, D. (1979) *Cell 18*, 93–100.

Gopalakrishnan, V., Peliska, J. A., & Benkovic, S. J. (1992) *Proc. Natl. Acad. Sci. U.S.A. 89*, 10763–10767.

Gorecki, M., & Panet, A. (1978) *Biochemistry 17*, 2438–2442.

Grandgenett, D. P., Gerard, G. F., & Green, M. (1972) *J. Virol. 10*, 1136–1142.

Hall, S. H., & Crouch, R. J. (1977) *J. Biol. Chem. 252*, 4092–4097.
Hansen, J., Schulze, T., Mellert, W., & Moelling, K. (1988) *EMBO J. 7*, 239–243.
Herr, W. *(1984) J. Virol. 49*, 471–478.
Hizi, A., McGill, C., & Hughes, S. H. (1988) *Proc. Natl. Acad. Sci. U.S.A. 85*, 1218–1222.
Hizi, A., Hughes, S. H., & Shaharabany, M. (1990) *Virology 175*, 575–580.
Hizi, A., Tal, R., & Hughes, S. H. (1991) *Virology 180*, 339–346.
Hostomsky, Z., Hostomska, Z., Hudson, G. O., Moomaw, E. W., & Nodes, B. R. (1991) *Proc. Natl. Acad. Sci. U.S.A. 88*, 1148–1152.
Hu, S. C., Court, D. L., Zweig, M., & Levin, J. G. (1986) *J. Virol. 60*, 267–274.
Huber, H. E., McCoy, J. M., Seehra, J. S., & Richardson, C. C. (1989) *J. Biol. Chem. 264*, 4669–4678.
Itaya, M., & Crouch, R. J. (1991) *MGG, Mol. Gen. Genet. 227*, 424–432.
Jacobo-Molina, A., & Arnold, E. (1991) *Biochemistry 30*, 6351–6361.
Johnson, M. S., McClure, M. A., Feng, D.-F., Gray, J., & Doolittle, R. F. (1986) *Proc. Natl. Acad. Sci. U.S.A. 83*, 7648–7652.
Kanaya, S., & Crouch, R. J. (1983) *J. Biol. Chem. 258*, 1276–1281.
Katayanagi, K., Miyagawa, M., Matsushima, M., Ishikawa, M., Kanaya, S., Ikehara, M., Matsuzaki, T., & Morikawa, K. (1990) *Nature 347*, 306–309.
Kati, W. M., Johnson, K. A., Jerva, L. F., & Anderson, K. S. (1992) *J. Biol. Chem. 267*, 25988–25997.
Keller, W., & Crouch, R. (1972) *Proc. Natl. Acad. Sci. U.S.A. 69*, 3360–3364.
Kohlstaedt, L. A., Wang, J., Friedman, J. M., Rice, P. A., & Steitz, T. A. (1992) *Science 256*, 1783–1790.
Kotewicz, M. L., Sampson, C. M., D'Alessio, J. M., & Gerard, G. F. (1988) *Nucleic Acids Res. 16*, 265–277.
Krug, M. S., & Berger, S. L. (1989) *Proc. Natl. Acad. Sci. U.S.A. 86*, 3539–3543.
Lai, M.-H.T., & Verma, I. M. (1978) *J. Virol. 25*, 652–663.
Lautenberger, J. A., Court, D., & Papas, T. S. (1983) *Gene 23*, 75–84.
Leis, J. P., Berkower, I., & Hurwitz, J. (1973) *Proc. Natl. Acad. Sci. U.S.A. 70*, 466–470.
Levin, J. G., Grimley, P. M., Ramseur, J. M., & Berezesky, I. K. (1974) *J. Virol. 14*, 152–161.
Levin, J. G., Crouch, R. J., Post, K., Hu, S. C., McKelvin, D., Zweig, M., Court, D. L., & Gerwin, B. I. (1988) *J. Virol. 62*, 4376–4380.
Luo, G., & Taylor, J. (1990) *J. Virol. 64*, 4321–4328.
Modak, M. J. (1976) *Biochem. Biophys. Res. Commun. 71*, 180–187.
Moelling, K. (1974) *Virology 62*, 46–59.
Moelling, K. (1976) *J. Virol. 18*, 418–425.
Moelling, K., Bolognesi, D. P., Bauer, H., Büsen, W., Plassmann, H. W., & Hausen, P. (1971) *Nature (London) New Biol. 234*, 240–243.
Oyama, F., Kikuchi, R., Crouch, R. J., & Uchida, T. (1989) *J. Biol. Chem. 264*, 18808–18817.
Peliska, J. A., & Benkovic, S. J. (1992) *Science 258*, 1112–1118.
Prasad, V. R., & Goff, S. P. (1989) *Proc. Natl. Acad. Sci. U.S.A. 86*, 3104–3108.
Restle, T., Müller, B., & Goody, R. S. (1992) *FEBS Lett. 300*, 97–100.
Schatz, O., Mous, J., & LeGrice, S. F. J. (1990) *EMBO J. 9*, 1171–1176.
Sisk, W. P., Chirikjian, J. G., Lautenberger, J., Jorcyk, C., Papas, T. S., Berman, M. L., Zagursky, R., & Court, D. L. (1986) *Gene 48*, 183–193.
Tan, C.-K., Zhang, J., Li, Z.-Y., Tarpley, W. G., Downey, K. M., & So, A. G. (1991) *Biochemistry 30*, 2651–2655.
Tanese, N., & Goff, S. P. (1988) *Proc. Natl. Acad. Sci. U.S.A. 85*, 1777–1781.
Telesnitsky, A., & Goff, S. P. (1993) *Proc. Natl. Acad. Sci. U.S.A. 90*, 1276–1280.
Telesnitsky, A., Blain, S. W., & Goff, S. P. (1992) *J. Virol. 66*, 615–622.
Varmus, H., & Swanstrom, R. (1984) in *Molecular Biology of Tumor Viruses, RNA Tumor Viruses* (Weiss, R., Teich, N., Varmus, H., & Coffin, J., Eds.) 2nd ed., pp 369–512, Cold Spring Harbor Laboratory Press, Cold Spring Harbor, NY.
Verma, I. M. (1975) *J. Virol. 15*, 843–854.
Wohrl, B. M., & Moelling, K. (1990) *Biochemistry 29*, 10141–10147.
Wohrl, B. M., Volkmann, S., & Moelling, K. (1991) *J. Mol. Biol. 220*, 801–818.
Yang, W., Hendrickson, W. A., Crouch, R. J., & Satow, Y. (1990) *Science 249*, 1398–1405.